ELSEVIER

Chemical Engineering Journal 89 (2002) 109–117

Chemical Engineering Journal

www.elsevier.com/locate/cej

Bubble size in aerated stirred tanks

S.S. Alves [a,*], C.I. Maia [a], J.M.T. Vasconcelos [a], A.J. Serralheiro [b]

[a] Centro de Engineering Biológica e Química, Department of Chemical Engineering, Instituto Superior Técnico, 1049-001 Lisboa, Portugal
[b] Department of Electrotechnical Engineering and Computers, Instituto Superior Técnico, 1049-001 Lisboa, Portugal

Received 1 August 2001; accepted 15 December 2001

Abstract

Local average bubble size in a dual turbine stirred tank is investigated. Results are compared with data from the literature, obtained under many different conditions, including different types and numbers of stirrers, different media and measuring systems. For Rushton turbines, bubble size increases from the stirrer tip along the discharge stream, soon to reach a value representative of the bulk of the tank, near the tank wall. This is common to coalescing and non-coalescing systems. Differences in d_{32} cannot be clearly attributed to size of tank, number or type of stirrers or measuring method. Dispersion within each author's data is at least as significant as the differences between authors. Bubble sizes in electrolyte solutions are smaller and more sensitive to power input than in water. Surfactant addition results in a further decrease in bubble size. Data may be correlated by $d_{32} = C''(P_g/V)^{\beta}$ with exponent β decreasing from (−0.52) near turbine to (−0.37) bulk for non-coalescing media and from (−0.24) near turbine to (−0.14) bulk for coalescing media. The effect of gas flowrate on d_{32} is not detectable, except near the turbine for coalescing media. To correlate data under these conditions, the effect of gas loading must be included.

Keywords: Bubble size; Aerated stirred tanks; Gas–liquid mass transfer

1. Introduction

Research on gas–liquid mass transfer in stirred tanks in the past has mostly concentrated on establishing correlations for the overall mass transfer coefficient. Not much information is available about either the mass coefficient, k_L, or the interfacial area, a. To be able to separate these and try to understand better the phenomena involved, data on bubble sizes in stirred tanks are required.

1.1. Experimental methods

Data on bubble sizes in stirred tanks are not abundant and little comparison is provided in the literature between the data available from various authors. A variety of methods have been used. Vermeulen et al. [1], Calderbank [2] and Lee and Meyrick [3], among others, obtained d_{32} by inference from gas hold-up, ε and interfacial area, a, determined by light attenuation methods. Figueiredo [4] used a four-element conductivity probe to measure both bubble diameter, velocity and flow direction, with a minimum detectable bubble diameter of 0.98 mm. Greaves and Kobbaci [5] and Barigou and Greaves [6,7] used suction probes. These were capillaries provided with light emission/detection, from which the bubble size was measured. Sensitivity was down to 0.3 mm bubble diameter. Kamiwano et al. [8] proposed a suction method coupled with high speed image processing. Parthasaray et al. [9] and Parthasarathy and Ahmed [10] drew gas–liquid samples through a thin cell where the bubbles were photographed. Takahashi and Nienow [11,12], Machon et al. [13], Martin [14] and Bouaifi and Roustan [15] have used non-intrusive photography/video techniques. Sensitivity was improved down to a minimum bubble diameter of 40 μm [13], but these visual methods may only take measurements near the tank wall, unless the gas hold-up is extremely small, as was the case with Takahashi and Nienow [11,12].

Comparison between the results obtained by the suction and video/photographic techniques has been carried out for a liquid–liquid dispersion by Pacek and Nienow [16], who found significant differences in the shape of the distribution, this being attributed to the limited range of the suction method. No comparison has been attempted in a gas–liquid situation.

1.2. Data correlation

Assuming that the breakage process in the turbulent flow controls bubble size, correlation of results is usually inspired

* Corresponding author. Tel.: +351-1-8417188; fax: +351-1-8499242.
E-mail address: salves@alfa.ist.utl.pt (S.S. Alves).

1385-8947/02/$ – see front matter © 2002 Elsevier Science B.V. All rights reserved.
PII: S1385-8947(02)00008-6

Nomenclature

C, C', C''	constants in Eqs. (1)–(3)
d_{10}	average bubble diameter, $d_{10} = \frac{\sum_{i=1}^{n} d_i}{n}$ (m)
d_{32}	surface based mean bubble diameter, $d_{32} = \frac{\sum_{i=1}^{n} {d_i}^3}{\sum_{i=1}^{n} {d_i}^2}$ (m)
$\bar{d}_B$	d_{32} for the bulk of the tank (1: lower half; 2: upper half; m)
d_{max}	maximum stable bubble diameter (m)
d_T	d_{32} produced by a turbine (1: lower turbine; 2: upper turbine; m)
D	turbine diameter (m)
N	agitation rate (s^{-1})
P_g	aerated turbine power (W)
Q	gassing rate ($m^3\,s^{-1}$)
v	air superficial velocity ($m\,s^{-1}$)
V	liquid volume (m^3)
V_I	impeller swept volume (m^3)

Greek symbols

α	gas hold-up
β	exponent in Eq. (4)
ε	turbulent energy dissipation rate per unit mass ($m^2\,s^{-3}$)
ρ	liquid density ($kg\,m^{-3}$)
σ	surface tension ($N\,m^{-1}$)

on a relationship theoretically developed by Hinze [17], for liquid dispersions. According to it, the disruptive forces acting on a bubble due to turbulent fluctuations are balanced by stabilizing surface tension forces. When the ratio of the two forces exceeds a critical value, the bubble breaks. Assuming Kolmogoroff's theory of isotropic turbulence, this leads to a maximum stable bubble diameter, d_{max}, given by [2]:

$$d_{max} = C\left(\frac{\sigma^{3/5}}{\varepsilon^{2/5}\rho^{3/5}}\right) \quad (1)$$

where σ is the surface tension, ρ the liquid density and ε is the energy dissipation rate per unit mass. A common assumption is that the Sauter mean diameter, d_{32}, is proportional to d_{max}, leading to

$$d_{32} = C'\left(\frac{\sigma^{3/5}}{\varepsilon^{2/5}\rho^{3/5}}\right) \quad (2)$$

On empirical grounds, Calderbank [2] extended Eq. (2), to include effects of gas hold-up:

$$d_{32} = C''\left(\frac{\sigma^{3/5}}{\varepsilon^{2/5}\rho^{3/5}}\right)\alpha^{1/2} \quad (3)$$

Most authors estimate ε as the impeller power per unit mass, $P_g/\rho V$. V is usually taken to be the liquid volume in the tank, although there is some debate as to whether the volume swept by the impeller, V_I, would not be more appropriate [9,10]. This leads to the following simplified version of Eq. (2), between the Sauter mean diameter and the ratio P_g/V:

$$d_{32} = C''\left(\frac{P_g}{V}\right)^{\beta} \quad (4)$$

Eqs. (1) and (2) are only valid if no coalescence occurs, leading to an exponent $\beta = -0.4$, but Eq. (4) has been used with a lower absolute value for exponent β (e.g. Pacek et al. [18], for liquid–liquid dispersions) to correlate data even when some coalescence has occurred.

In this work, the suction method developed by Greaves and Kobbacy [5], is used to determine local bubble size distributions in an aerated tank stirred by two Rushton turbines. Data is then compared in a systematic way with data from the literature, obtained under many different conditions, including different types and numbers of stirrers, different media and measuring systems.

2. Experimental

The experimental set-up consisted of a 0.292 m diameter, flat-bottomed, fully baffled Perspex vessel. Agitation was

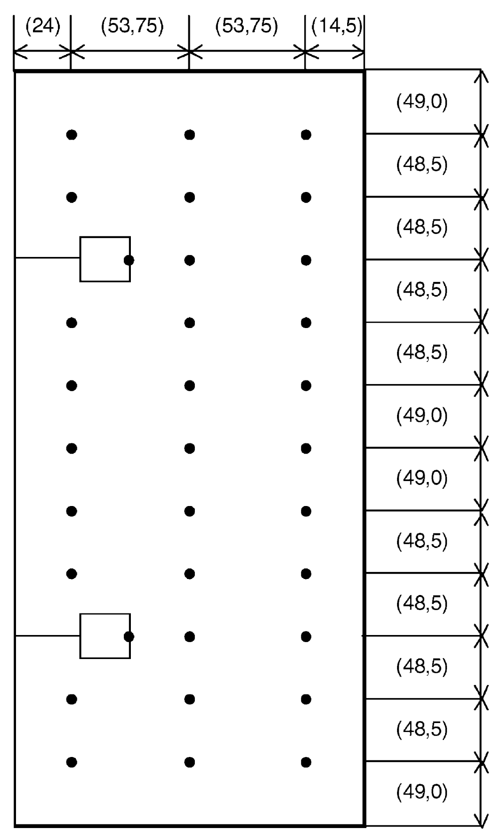

Fig. 1. Location of experimental sampling points (●) in mid-plane between two baffles. Distances in mm.

provided by two 0.096 m standard Rushton turbines set at distances of 0.146 and 0.438 m, respectively, above the tank base.

For local bubble size distributions, the technique developed by Barigou and Greaves [6], was used. It involves withdrawing, by means of a vacuum system, a continuous stream of gas–liquid dispersion through a short length calibrated capillary, 0.3 mm in diameter. Gas bubbles are transformed into elongated slugs inside the capillary, which are then detected by a pair of LED phototransistors. Iso-kinetic sampling being a major issue in this method, it has been dealt with by using a sample flow rate according to the criterion of the maximum local gas hold-up condition [5]. The bubble diameter detection limit is determined by capillary diameter, thus approximately 0.3 mm. Location of the sampling points is shown in Fig. 1.

All experiments were carried out in the vertical mid-plane between two adjacent baffles, for agitation rates of 5 and $7.5\,s^{-1}$, air flow rate of 1.67×10^{-4} and $3.34\times10^{-4}\,m^3\,s^{-1}$ (0.25 and 0.5 vvm based on the whole tank) and a total liquid height of 0.584 m. The liquid media used were tap water, a 0.3 M aqueous solution of sodium sulfate and 0.3 M aqueous solution of sodium sulfate with 20 ppm PEG.

3. Results and discussion

3.1. Structure of the dispersion

Fig. 2 shows maps of local Sauter mean bubble diameters, d_{32}, for a dual Rushton turbine agitated tank, in both non-coalescing liquid media and in tap water. It confirms a situation already revealed by the results of Barigou [19] and Barigou and Greaves [7], for a single turbine tank, namely, that average bubble size increases quickly in the turbine discharge stream and then reaches a "bulk value," which is roughly constant for the rest of the tank. This is illustrated in Fig. 3(a) and (b), for single and double turbine tanks, respectively. The Sauter mean diameter locally produced by the turbine will be referred as d_T, while the bulk-averaged Sauter mean diameter will be represented by $\bar{d}_B$.

Fig. 3(a) is representative of the situation found in Barigou and Greaves' data obtained with a single Rushton turbine stirred tank filled with tap water [7,19]. Most of the coalescence is completed by the time the discharge stream reaches the wall, although a small amount of coalescence still occurs upwards and downwards close to the tank wall. Fig. 3(a) is qualitatively compatible with data by the same authors for an aqueous salt solution and also with data by Takahashi et al. [12] for distilled water. Parthasarathy et al. [9] also reported that bubble size does not change throughout the tank by more than 10% for a non-coalescing medium.

Fig. 3(b) is representative of the situations described in detail in Fig. 2, i.e. for a double Rushton turbine stirred tank, both with coalescing and non-coalescing liquid media. Two values of d_T are found, one for each turbine. $d_{T_1} > d_{T_2}$, since there is a larger power dissipation in the upper turbine. The same happens for the bulk values, i.e. $\bar{d}_{B_1} > \bar{d}_{B_2}$, although the difference is much less significant. Some regions of exception are found, namely:

- (i) below the bottom turbine and in a small region just above it, where only small bubbles with low buoyancy follow the downward liquid circulation stream, particularly at low turbine speeds. This leads to lower average bubble sizes and lower gas hold-ups;
- (ii) near the wall, just below the turbine discharge streams, where upcoming bubbles from the lower part of the tank meet the downcoming half of the upper turbine discharge stream, promoting coalescence;
- (iii) near the surface, at the center of the tank, probably due to surface entrainment.

Although on average slightly smaller than $\bar{d}_B$, results near the tank wall may be accepted as an approximation to the average bulk value, making it possible to compare video and photographic data from recent studies, both with each other and with results obtained using the suction method.

3.2. Bubble size in the bulk of the tank

3.2.1. Non-coalescing systems: electrolyte solutions

Fig. 4(a) brings together data from several authors on $\bar{d}_B$ for electrolyte solutions. These were obtained by several methods, at several locations, for several types of stirrer, different sizes and numbers of stirrers, as presented in Table 1. Data from [7,19] were not included since the electrolyte concentration used (0.15 M of NaCl), although retarding coalescence, is not sufficient to produce a clearly non-coalescing medium [20,21,22,23].

Dispersion in the data is quite large, large in fact within each authors' data, masking any differences between authors. Thus, nothing may be concluded about the effect of impeller type, even though Martin [14] used a Prochem Maxflo impeller, while both Machon et al. [13] and this work used Rushton turbines. Nor may any clear difference be attributed to the detection method, even though the present work used the suction method, which is "blind" to bubbles smaller than ∼300 μm, while both Machon et al. [13] and Martin [14] used the video technique. This agreement is not totally surprising, since the very small bubbles, while affecting the arithmetic mean diameter, d_{10}, hardly affect the Sauter mean diameter, d_{32}, for the range of diameters at play [24].

The one factor that appears to affect $\bar{d}_B$ is electrolyte concentration, which is responsible for the dispersion within the data of Machon et al. [13] for the same P_g/V. This might be surprising in the light of experimental coalescence data in stagnant liquids [20,23], which suggest a very sharp change from a coalescing to non-coalescing situation as electrolyte concentration increases. On the other hand the data by Machon et al. [13] and those by Kietel and Onken [21,22] for bubble columns suggest that the effect of electrolyte

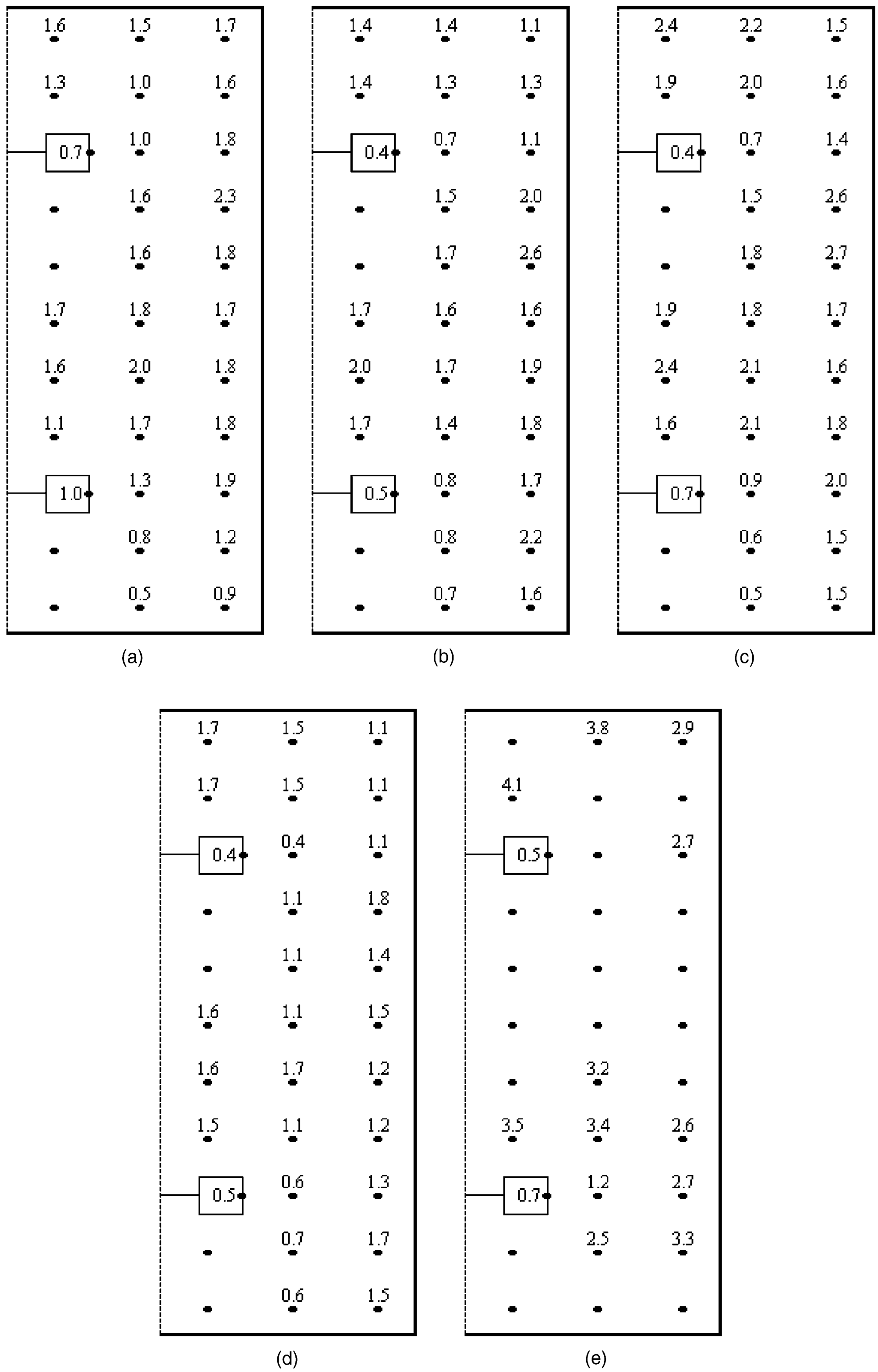

Fig. 2. Local Sauter mean bubble diameters: (a) aqueous Na_2SO_4, 0.3 M solution, $N = 5\,s^{-1}$, $Q = 1.67 \times 10^{-4}\,m^3\,s^{-1}$; (b) aqueous Na_2SO_4, 0.3 M solution, $N = 7.5\,s^{-1}$, $Q = 1.67 \times 10^{-4}\,m^3\,s^{-1}$; (c) aqueous Na_2SO_4, 0.3 M solution, $N = 7.5\,s^{-1}$, $Q = 3.34 \times 10^{-4}\,m^3\,s^{-1}$; (d) aqueous Na_2SO_4, 0.3 M with 20 ppm PEG, $N = 7.5\,s^{-1}$, $Q = 1.67 \times 10^{-4}\,m^3\,s^{-1}$; (e) tap water, $N = 7.5\,s^{-1}$, $Q = 1.67 \times 10^{-4}\,m^3\,s^{-1}$.

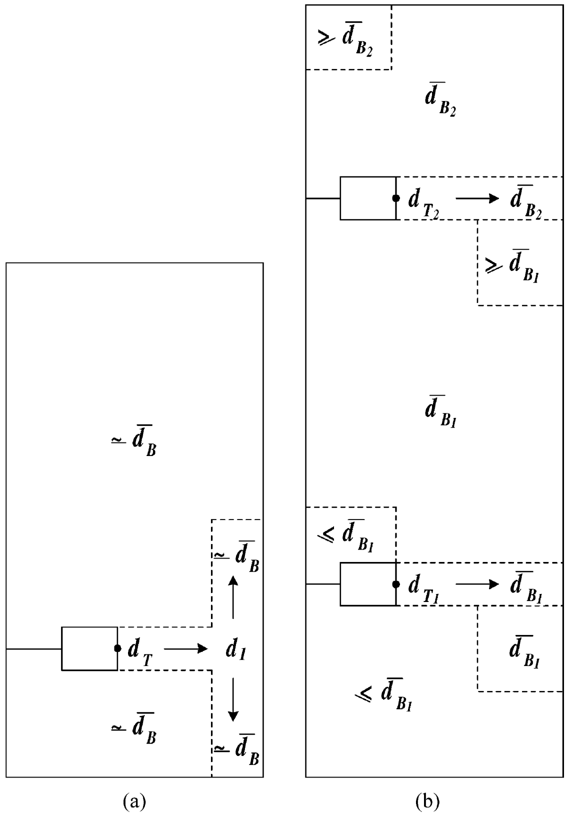

Fig. 3. Typical spatial distribution of mean diameters for a tank stirred by (a) a single Rushton turbine, and (b) two Rushton turbines.

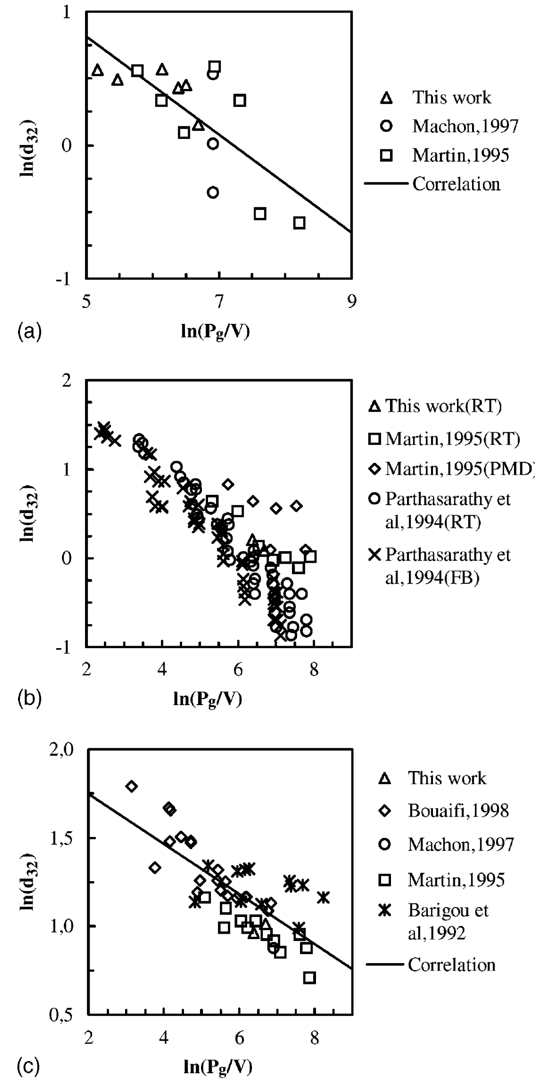

Fig. 4. Sauter mean bubble diameter (average for the bulk of the tank) as a function of power input per unit tank volume: (a) electrolyte solutions; (b) aqueous media with surfactant addition (RT: Rushton turbine; PMD: Prochem Maxflo T; FB: flat blade; (c) water.

concentration on bubble size under liquid dynamic conditions is more gradual.

Despite the dispersion, a correlation was established for the data in Fig. 4(a):

$$\bar{d}_B = 0.014 \left(\frac{P_g}{V}\right)^{-0.37} \tag{5}$$

The exponent is in reasonable agreement with Eq. (4), assuming that the turbulent energy dissipation ε may be given by $P_g/\rho V$ in the bulk of the tank.

3.2.2. Non-coalescing systems: surfactant addition

Fig. 4(b) displays data on $\bar{d}_B$ for aqueous systems with surfactant addition. Clearly the dispersion in the data is high and related to type and/or concentration. Martin [14] added 5 ppm of PPG, obtaining the largest bubbles for the same power input and the smallest sensitivity of $\bar{d}_B$ on P_g/V ($\beta = -0.28$), implying a higher degree of coalescence. The present work involved addition of 20 ppm of PEG, resulting in an intermediate value of $\bar{d}_B$, while Parthasarathy et al. [9] and Parthasarathy and Ahmed [10] added 50 ppm of methyl isobutyl carbinol to obtain the smallest bubbles and the highest sensitivity of $\bar{d}_B$ on P_g/V ($\beta = -0.48$). However, the fact that each work used a different additive does not allow separating the effects of type and concentration of surfactant.

What is clear is that addition of tensioactive materials tends to decrease bubble size, as shown in Fig. 5, which sums up trends for all types of liquid systems under study. The effect of impeller is not very significant in either the work of Parthasarathy et al. [9] and Parthasarathy and Ahmed [10] or that of Martin [14], although the Rushton turbine appears to produce slightly smaller bubbles than the other types of impeller.

3.2.3. Coalescing systems

Fig. 4(c) brings together data from several authors on $\bar{d}_B$ for coalescing media. Table 1 again presents some details about the differences between the sources of these data. Data by Takahashi and Nienow [12] were not included because P_g/V is not available, although a rough estimation of this

Table 1
Research on bubble size in stirred tanks

Authors	Tank diameter (m)	Impeller type and number	Measuring technique	Sampling position	Systems studied	Gas superficial velocity (m s^{-1})
Barigou [19]	1.0	Single: RT	Photoelectric suction probe	Throughout the tank	Air–water	0.0021–0.0088
Martin [14]	0.56	Single: RT, PMD	Video	Near wall, mid-height	Air–water; air–Na_2SO_4, 0.2 M; air–water + 5 ppm PPG	0.0093
Machon et al. [13]	0.15	Single: RT	Video	Near wall, Z=0.78H	Air-water; air-Na_2SO_4, 0.2 M; air–Na_2SO_4, 0.5 M; air–Na_2SO_4, 1.0 M	0.0028
Bouaifi and Roustan [15]	0.43	Double: 2 × A315, A315 + A310, A315 + PBTD	Video	Near wall, avg. of 3 heights	Air–water	0.0036–0.011
Present work	0.29	Double: RT	Photoelectric suction probe	Throughout the tank	Air–water; air–Na_2SO_4, 0.3 M; air–water + 5 ppm PPGin Na_2SO_4, 0.3 M	0.0025–0.0050
Parthasarathy et al. [9,10]	0.195	Single: RT, FB, MP, PBD, PBU	Suction followed by photography	Middle radius, mid-height	Air–water + 50 ppm, methyl isobutyl carbinol	0.00025–0.0012

RT: Rushton turbine; PMD: Prochem Maxflo T; A310, A315: lightnin axial flow impellers; FB: flat blade turbine; PB: pitched blade turbine; PBU, PBD: upward, downward pumping pitched blade turbine; MP: marine propeller; Z: distance from bottom; H: liquid height.

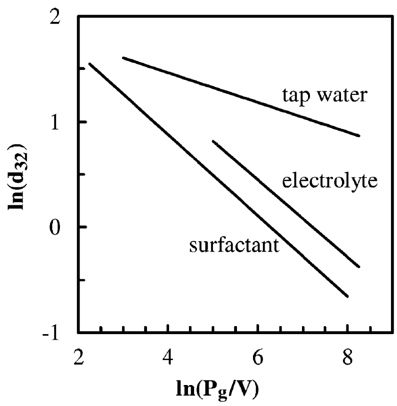

Fig. 5. Sauter mean bubble diameter (average for the bulk of the tank) as a function of power input per unit tank volume; comparison for three types of liquid media.

parameter allows to state that these authors' results would also fit reasonably well.

As shown in Fig. 5, diameters are higher than those obtained with non-coalescing systems. Data are reasonably well correlated by the expression:

$$\bar{d}_B = 0.0076\left(\frac{P_g}{V}\right)^{-0.14} \quad (6)$$

The exponent on P_g/V, -0.14, no longer agrees with considerations from turbulence theory, being quite smaller, as had been commented in the literature, e.g. [13,18]. This means that bubble size in the bulk of the tank is strongly influenced by coalescence, the effect of turbulence on bubble formation having already been diluted by other factors. Dispersion in the data is smaller than with non-coalescing systems and Eq. (6) may be used to predict bubble size within a 25% error, for a 95% confidence level. No hint of any influence of impeller type may be found in these data.

3.3. Bubble size at the turbine discharge

Fig. 6 shows how average bubble size very near the turbine discharge varies with P_g/V_I for various gas loadings, where V_I is the impeller swept volume. P_g/V_I is used instead of P_g/V to correlate data, since it expresses better the turbulent energy dissipation at this location. Fig. 6 brings together original data for the double turbine tank described in the experimental section and data from Barigou and Greaves [7]. Data in Fig. 6 were obtained 48 mm away from the tip of the impeller in the 1 m diameter tank of Barigou and Greaves [7,25] and 25 mm away in the 0.29 m diameter tank of the present work. Two main facts emerge, as follows:

(i) All data for non-coalescing systems, both obtained by addition of electrolyte or PEG, as well as data for coalescing system at low gas loading (~0.002 $m\,s^{-1}$ superficial velocity for all data) can be correlated by a single expression:

$$d_T = 0.25\left(\frac{P_g}{V_I}\right)^{-0.52} \quad (7)$$

This suggests that neither electrolyte nor surfactant significantly affect the process of bubble formation, but only the subsequent coalescence process. The exponent found is larger than theoretically suggested by Eq. (4). It is not clear whether this is due to experimental error or to theoretical inadequacy.

(ii) For coalescing systems, the effect of gas loading becomes important. Since the transition point from

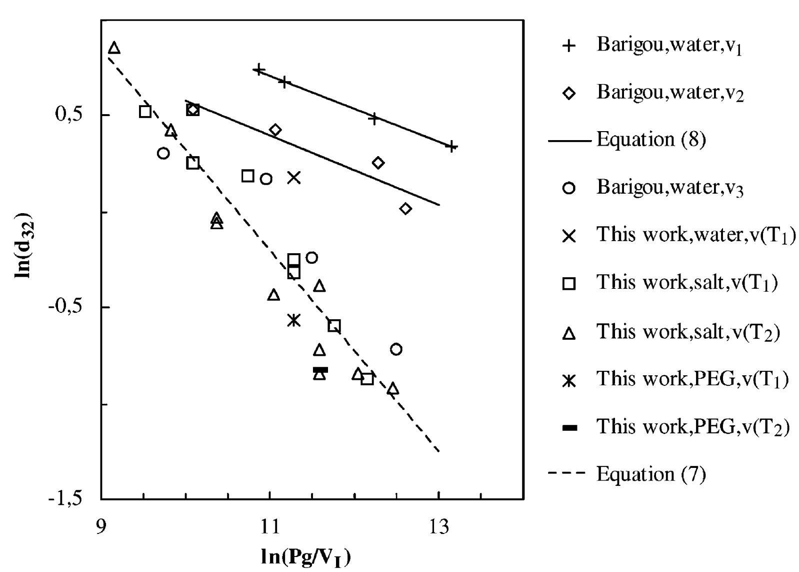

Fig. 6. Sauter mean bubble diameter at turbine discharge as a function of power input per unit impeller swept volume, for different liquid media. Air superficial velocity: $v_1 = 0.0088\,m\,s^{-1}$; $v_2 = 0.0056\,m\,s^{-1}$; $v_3 = 0.0021\,m\,s^{-1}$; $v(T_1)$ (single turbine) $= v(T_2)$ (dual turbine) $= 0.0025\,m\,s^{-1}$.

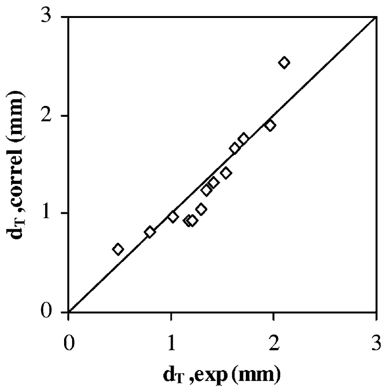

Fig. 7. Comparison between experimental and predicted (Eq. (8)) Sauter mean bubble diameter at turbine discharge. Data from Barigou [19] and this work.

clinging to "3–3" large cavities, as defined by Smith and Warmoeskerken [26], is passed across the range of gas flow numbers covered, this suggests that the ventilated cavities structure and dimensions play an important role in the size of the bubbles. This could also substantiate the link between turbine power dissipation and turbine bubble size, as commented about d_{T_1} and d_{T_2} in Fig. 3(b). Calderbank's Eq. (3) or an analogous expression involving gas hold-up could not be used to correlate the whole data, since gas hold-up in the impeller region is unknown. An expression involving another measure of gas loading, namely Q/D^2, was used with good results, as shown in the parity diagram of Fig. 7, namely:

$$d_T = 8.5\left(1 + 32.5\frac{Q}{D^2}\right)\left(\frac{P_g}{V_l}\right)^{-0.24} \quad (8)$$

4. Conclusions

(i) In an aerated stirred tank, bubble size increases quickly in the turbine discharge stream and then reaches a "bulk value", which is roughly constant for the rest of the tank.

(ii) Comparison between data from several authors on bubble diameter is possible so long as data in roughly the same relative location in the tank are used in the comparison.

(iii) Differences in d_{32} cannot be clearly attributed to size of tank, number or type of stirrers, or measuring method. Dispersion within each author's data is at least as significant as the differences between authors.

(iv) Bubble sizes in electrolyte solutions are smaller and more sensitive to power input than in water. Surfactant addition results in a further decrease in bubble size. Data also suggest that type and/or concentration of both electrolyte and surfactant added may affect bubble size.

(v) Data may be correlated by $d_{32} = C''(P_g/V)^{\beta}$. Exponent β decreases from (−0.52) near turbine to (−0.37) bulk for non-coalescing media and from (−0.24) near turbine to (−0.14) bulk for coalescing media, as d_{32} becomes more and more influenced by coalescence, the effect of turbulence on bubble formation being diluted by other factors.

(vi) The effect of aeration on d_{32} is not detectable, except near the turbine for coalescing media. To correlate data under these conditions, the effect of gas loading must be included.

Acknowledgements

Financial support by PRAXIS XXI, Project no. 2/2.1/BIO/1061/95 and the research Grant awarded to C.I. Maia (PRAXIS XXI 4/4.1/BD/2935/96) are also gratefully acknowledged.

References

[1] T. Vermeulen, G.M. Williams, G.E. Langlois, Interfacial area in liquid–liquid and gas–liquid agitation, Chem. Eng. Progr. 51 (1955) 85F–94F.
[2] P.H. Calderbank, The interfacial area in gas–liquid contacting with mechanical agitation, Trans. Instrum. Chem. Eng. 36 (1958) 443–463.
[3] J.C. Lee, D.L. Meyrick, Gas–liquid interfacial areas in salt solutions in an agitated tank, Trans. Instrum. Chem. Eng. 48 (1970) T37–T45.
[4] M. M. L. Figueiredo, The Physical and Mass Transfer Properties of Gas Dispersins in Mixing Vessels, PhD Thesis, University of Edinburgh, UK, 1978.
[5] M. Greaves, K.A.H. Kobbacy, Measurement of bubble size distribution in turbulent gas–liquid dispersions, Trans. Instrum. Chem. Eng. 62 (1984) 3–12.
[6] M. Barigou, M. Greaves, A capillary suction probe for bubble size measurement, Meas. Sci. Technol. 2 (1991) 318–326.
[7] M. Barigou, M. Greaves, Bubble size distributions in a mechanically agitated gas–liquid contactor, Chem. Eng. Sci. 47 (1992) 2009–2025.
[8] M. Kamiwano, M. Kaminoyama, K. Nishi, D. Shirota, A method for measuring bubble diameter distribution in gas–liquid agitated vessel under high gas hold-up using real-time high-speed image processing system, J. Chem. Eng. Jpn. 31 (1998) 366–373.
[9] R. Parthasarathy, G.J. Jameson, N. Ahmed, Bubble breakup in stirred vessels—predicting the Sauter mean diameter, Trans. Instrum. Chem. Eng. 69 (1991) 295–301.
[10] R. Parthasarathy, N. Ahmed, Sauter mean and maximum bubble diameters in aerated stirred vessels, Trans. Instrum. Chem. Eng. 72 (1994) 565–572.
[11] K. Takahashi, A. W. Nienow, Bubble sizes, gas hold-up and coalescence rates in aerated vessels agitated by a Rushton turbine: spatial variations, in: Proceedings of the 6th European Conference on Mixing, Pavia, Italy, 1988, pp. 285–292.
[12] K. Takahashi, A.W. Nienow, Bubble size distributions in an aerated vessel agitated by a Rushton turbine, J. Chem. Eng. Jpn. 26 (1993) 536–542.
[13] V. Machon, A.W. Pacek, A.W. Nienow, Bubble sizes in electrolyte and alcohol solutions in a turbulent stirred vessel, Trans. Instrum. Chem. Eng. 75 (1997) 339–348.
[14] T. Martin, Gas Dispersion with Radial and Hydrofoil Impellers in Fluids with Different Coalescence Characteristics, PhD Thesis, Birmingham University, Birmingham, 1995.
[15] M. Bouaifi, M. Roustan, Bubble size and mass transfer coefficients in dual-impeller agitated reactors, Can. J. Chem. Eng. 76 (1998) 390–397.

[16] A.W. Pacek, A.W. Nienow, Measurement of drop size distributions in concentrated liquid–liquid dispersions: video and capillary techniques, Trans. Instrum. Chem. Eng. 73 (1995) 512–518.
[17] J.O. Hinze, Fundamentals of the hydrodynamic mechanism of splitting dispersion process, AIChE J. 1 (1955) 289–295.
[18] A.W. Pacek, C.C. Man, A.W. Nienow, On the Sauter mean diameter and size distributions in turbulent liquid–liquid dispersions in a stirred vessel, Chem. Eng. Sci. 53 (1998) 2005–2011.
[19] M. Barigou, Bubble size, gas hold-up and interfacial area distributions in mechanically agitated gas–liquid reactors, PhD Thesis, The University of Bath, UK, 1987.
[20] R.R. Lessard, S.A. Zieminski, Bubble coalescence and gas transfer in aqueous electrolytic solutions, Ind. Eng. Chem. Fundam. 10 (1971) 260–269.
[21] G. Keitel, U. Onken, The effect of solutes on bubble size in air–water dispersions, Chem. Eng. Commun. 17 (1982) 85–98.
[22] G. Keitel, U. Onken, Inhibition of bubble coalescence by solutes in air–water dispersions, Chem. Eng. Sci. 37 (1982) 1635–1638.
[23] T.O. Oolman, H.W. Blanch, Bubble coalescence in stagnant liquids, Chem. Eng. Commun. 43 (1986) 237–261.
[24] J.H. Bae, L.L. Tavlarides, Laser capillary spectrophotometry for drop size concentration measurements, AIChE J. 35 (1989) 1073–1084.
[25] M. Barigou, M. Greaves, Bubble size in the impeller region of a Rushton turbine, Trans. Instrum. Chem. Eng. Part A 70 (1992) 153–160.
[26] J.M. Smith, M.M.C.G. Warmoeskerken, The dispersion of gases in liquids with turbines, in: Proceedings of the 5th European Conference on Mixing, Wurzburg, Germany, 1985, pp. 115–126.